이 학 석 사 학 위 논 문

Determination of the flow rate and mixing ratio of the Changjiang diluted water in surface seawater of the northwestern Pacific marginal seas using radium isotopes

한반도 주변해 표층수중 라듐 동위원소를 이용한 양자강 희석수의 유출속도 및 혼합비율 측정

2014년 2월

서울대학교 대학원

지 구 환 경 과 학 부

이 호 준

Determination of the flow rate and mixing ratio of the Changjiang diluted water in surface seawater of the northwestern Pacific marginal seas using radium isotopes

한반도 주변해 표층수중 라듐 동위원소를 이용한
양자강 희석수의 유출속도 및 혼합비율 측정

지도교수 김 규 범

이 논문을 이학석사 학위논문으로 제출함

2013년 10월

서울대학교 대학원
지구환경과학부
이 호 준

이호준의 석사학위논문을 인준함
2013년 12월

위 원 장 조 양 기 (인)

부 위 원 장 김 규 범 (인)

위 원 이 강 근 (인)

Abstract

Determination of the flow rate and mixing ratio of the Changjiang diluted water in surface seawater of the northwestern Pacific marginal seas using radium isotopes

Hojun Lee
School of Earth and Environmental Sciences
The Graduate School
Seoul National University

Ra isotopes (^{223}Ra and ^{228}Ra) in surface seawater of the northwestern Pacific marginal seas, including the East China Sea, southern sea of Korea, and the Yellow Sea, were measured to estimate the flow rate and to calculate the relative contribution of the Changjiang diluted water (CDW) during the summer season. On the basis of the horizontal distribution of ^{223}Ra activities, current speed of the CDW from the river mouth to 450 km offshore northeast was estimated to be 16 ± 1 cm/s,

which was similar to that determined in previous studies that used physical methods such as surface drifter buoys and numerical modeling. Moreover, the relative contributions of CDW at each sampling station were calculated using mass balance equations for the salinity and ^{228}Ra activity. The relative contribution of CDW in surface water was more than 50% in most area of the northern East China Sea, the Yellow Sea, and even about 30% to the Korea/Tsushima Strait, which is approximately 800 km from the river mouth. These results suggest that CDW can be of high significance in the biogeochemistry of surface water of these northwestern Pacific marginal seas during the summer monsoon period.

Key words: Ra isotopes; Changjiang diluted water (CDW); current speed; Water mass mixing

***Student number*: 2012-22511**

Table of contents

List of tables

List of figures

1. Introduction

The northwestern Pacific marginal seas, including the largest continental shelf in the world, have received much attention from oceanographers since they are influenced by the input of large amount of freshwater from the Changjiang River and have highly complicated and dynamic current systems (Cho et al., 2009; Kim et al., 2013) (Figure 1). Among the seas, the northern East China Sea directly receives large amount of fresh water (annual mean discharge of 0.9×10^{12} m^3/y) from the Changjiang River (Gu et al., 2012). The Changjiang River water contains relatively high DIN (high N:P ratios up to 100-150), total suspended matter (up to 500-1,000 mg/L or higher), total dissolved solid (154×10^6 tons/y, second largest in the world), and other chemical species (Wong et al., 1998; Chen et al., 2002; Zhang, 2002).

However, Changjiang diluted water (CDW) is much different from the linear mixing between the river water and Kuroshio water, in terms of chemical and biological water properties, since there are vigorous biogeochemical reactions, such as desorption or adsorption of chemical species, and biological production in the estuarine mixing zone (Elsinger and Moore, 1984; Edmond et al., 1985). In general, CDW is formed along the Jiangsu and Zhejiang coasts and defined as water with salinity<32, although the upper limit of salinity differs slightly (Lie et al., 1984; Chang and Isobe, 2003).

Considering that the river plume moves even to hundreds of km into the open ocean, CDW has significant impact on the biogeochemistry of neighboring seas, such as the Yellow Sea and the southern sea of Korea, as well as the northern East China Sea (Moore et al., 2004). Using satellite-observed concentrations of

chlorophyll-a in the East China Sea, Kim et al. (2009) revealed that the distributions of CDW corresponded well with the area, showing the chlorophyll-a concentration to be more than 0.48 mg/m^3. Thus, studying the transport and mixing of CDW is important for understanding the biogeochemistry of this marginal sea.

Many studies have been conducted to determine the behaviors of CDW in this region by physical methods such as numerical modeling, surface drifter buoy, and satellite imagery (Lie et al., 2003; Kim et al., 2009; Moon et al., 2009). The spread of CDW into the surrounding seas was found to be most active from July to August on the basis of a three-dimensional numerical model, CTD data, and drifter trajectories (Lie at al., 2003; Moon et al., 2009). The flow pattern of CDW over this continental shelf is largely dependent on the surface wind directions, predominant northward wind in summer and southward wind in winter, causing Ekman transport of freshwater eastward or westward, respectively (Lie et al., 2003; Moon et al., 2009). Lie et al. (2003) reported that mean current speeds of CDW from the northeast of river estuary to eastward were determined to be approximately 11-12 cm/s and 22-28 cm/s during the summers of 1997 and 1998, respectively, using satellite-tracked drifters.

However, it is hard to determine the quantitative amount of CDW emptying into surrounding seas using these physical methods. A drifter buoy method, which is a powerful but expensive technique for estimating current speeds, is limited in the shelf sea because of intensive fishing activities (Ichikawa and Beardsley, 2002). In addition, current speeds of CDW revealed by a drifter buoy technique cannot cover the whole area of CDW because of limited number of buoys.

In this regard, Ra isotopes (^{223}Ra, $t_{1/2}$ = 11.4 days; ^{224}Ra, $t_{1/2}$ = 3.6 days;

^{226}Ra, $t_{1/2}$ = 1,622 years; and ^{228}Ra, $t_{1/2}$ = 5.75 years), which are naturally occurring U-Th series radionuclides, can be used as good tracers of the flow rate and mixing processes of CDW. Major input pathway of radium isotopes to the coastal ocean is desorption, which occurs when radium-absorbed riverine particles or suspended sediments meet high ionic strength seawater (Li et al., 1977; Elsinger and Moore, 1980; Moore, 2000). Once Ra isotopes input to the ocean, they are changed only by radioactive decay and mixing (Zhang et al., 2007).

One of the major source of radium in this continental shelf sea could be the Changjiang River plume since high sediment loading occurs during the summer flooding season (Milliman et al., 1985). Thus, the objectives of this study are (1) to determine the flow rate of CDW from the Changjiang River mouth to northeastward toward the vicinity of Jeju Island (~450 km) using the horizontal distribution of ^{223}Ra ($t_{1/2}$ = 11.4 days) activities and (2) to estimate the relative contributions of CDW in this complex and dynamic marginal sea using mass balance equations for ^{228}Ra ($t_{1/2}$ = 5.75 years) and salinity.

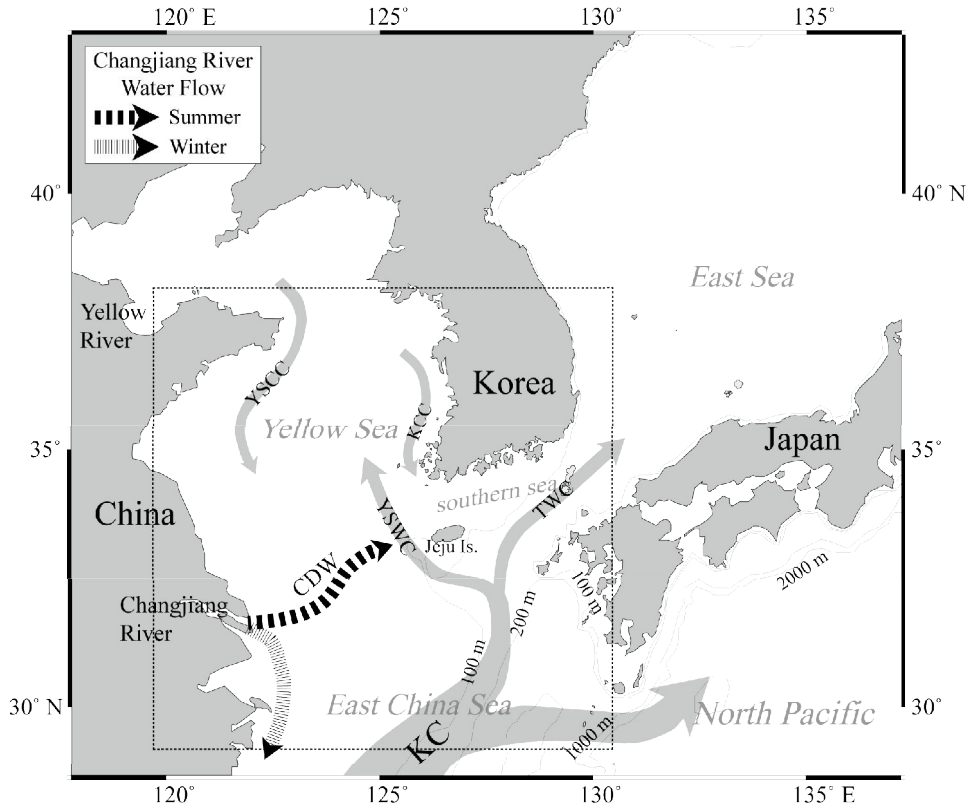

Figure 1. The northwestern Pacific marginal seas, which contains highly complicated and dynamic current systems, such as Kuroshio Current (KC), Korean Coastal Current (KCC), Yellow Sea Coastal Current (YSCC), Yellow Sea Warm Current (YSWC), and Tsushima Warm Current (TWC).

2. Materials and Methods

2.1 Study area and Sampling

The study region is located in the northwestern Pacific, including the East China Sea, the southern sea of Korea, and the Yellow Sea, which has the largest continental shelf in the world (Figure 2). Among the seas, the East China Sea has the widest area, approximately 9×10^5 km^2, with a mean depth of 188 m (Tsunogai et al., 1997). In the Yellow Sea, total area is 4×10^5 km^2, with a mean depth of 50 m. The southern sea of Korea has a relatively small area of 0.75×10^5 km^2, with a mean depth of 100 m (Kim et al., 2005).

The Changjiang River is the major source of fresh water in the study region because other rivers along the shoreline of China and the Korean Peninsula, such as the Yalu, Jiao, Han, and the Keum rivers, are much smaller (Chen et al., 1994). The current system is composed of perpetually northward flowing Taiwan Warm Current (TWC), Kuroshio Current (KC), Yellow Sea Warm Current (YSWC), Korean Coastal Current (KCC), and Yellow Sea Coastal Current (YSCC) (Kim et al., 2005) (Figure 1). On this continental shelf, the mean residence time of the Yellow Sea is approximately 5-6 years, whereas that of the East China Sea is relatively short (2-3 years) (Nozaki et al., 1991; Kim et al., 2005).

Surface (<3m) seawater samples for Ra were collected from the East China Sea (n = 27) during August 11 to 13, 2012, using the research vessel, *Tamgu-3*, of the National Fisheries Research and Development Institute (NFRDI), and from the Yellow Sea (n = 6) during August 13 to 14, 2012, using the *Badaro*, a Korea Coast Guard vessel in the 3,000-ton class. Samples from the southern sea of

Korea were obtained from August 21-22 (n = 18) and September 1-4 (n = 29), 2012, using *Tamgu-8* of the NFRDI before and after Typhoon 'Bolaven' (Figure 2).

Surface water samples of ~100 L were collected in polypropylene cubitainers by using a ship-installed pump. They were then passed through MnO_2-impregnated acrylic fiber (dry, ~16 g) column (4 cm diameter, 15 cm length) at a flow rate of <1.5 L min^{-1}, which is suitable for adsorbing Ra quantitatively onto the fiber (Kim et al., 2005).

2.2 Measurements of temperature and salinity

Salinities and temperatures in surface seawater of the East China Sea, the southern sea of Korea, and the Yellow Sea were measured directly using a CTD (Sea-Bird Electronics SBE-911+) instrument.

2.3 Analysis of Ra isotopes

2.3.1. ^{223}Ra and ^{224}Ra

The activities of ^{223}Ra and ^{224}Ra are measured using a radium delayed coincidence counter (RaDeCC, Scientific Computer Instruments, USA) system (Moore and Arnold, 1996) (Figure 4). Before measurements, Ra-adsorbed Mn-fibers were washed by using de-ionized water for removing any salts, and adjusted to wet weight of ~32 g (1:1 ratio of water and fiber) by hand-squeezing to create an optimal moisture condition for the emanation efficiency of ^{219}Rn and ^{220}Rn, daughters of ^{223}Ra and ^{224}Ra (Sun and Torgersen, 1998; Kim et al., 2001; Dulaiova and Burnett, 2004). Thereafter, water-content-adjusted Mn-fibers were stuffed in a

plastic column (4.5 cm diameter, 25 cm length) and it was connected to the air loop of RaDeCC system (Giffin et al., 1963; Moore and Arnold, 1996). The flow rate was adjusted to ~6 L/min (Moore and Arnold, 1996; Garcia-Solsona et al., 2008). Each sample was measured for 4-8 hours. Between each measurement, air loop system was purged with ambient air for at least 30 min to exclude the effects of Rn remaining in the counting cell (Garcia-Solsona et al., 2008).

For calibration of the RaDeCC system, two blank Mn-fibers and one standard Mn-fiber (^{223}Ra: 10.8 dpm, ^{224}Ra: 30.26 dpm) which was calibrated by FSU were used. Blank Mn-fibers were prepared by passing radium-free seawater (~500 mL) through Mn-fiber columns several times for quantitative adsorption of radium onto the Mn-fiber (Scholten et al., 2010).

The counting error of Ra isotopes is determined by following equation.

$$e = \frac{\sqrt{n}}{t}$$

where e is the counting error, n is the decay count of radionuclides , and t is the measurement time. Increasing the measurement time is needed to reduce the counting error. Averaged propagated error of ^{223}Ra activity was comparatively high (37%) since the activity of ^{223}Ra in natural seawater is extremely low, whereas that of ^{224}Ra activity was 12% (Kim et al., 2001). Counting efficiencies of ^{223}Ra and ^{224}Ra were 6% (n = 5) and 18% (n = 5).

2.3.2 ^{226}Ra and ^{228}Ra analysis

After the measurements of short-lived ^{223}Ra and ^{224}Ra isotopes, Mn-fiber

samples were ashed in a muffle furnace at 820°C for 16 hours (Charette et al., 2001). The ashes were sealed into gamma vials for 3 weeks to create a secular equilibrium between radium and its gamma-daughters (Kim et al., 2003). Ashed Mn-fiber samples were measured for 1-4 days using a well-type gamma spectrometer (Kim et al., 2003) (Figure 5). The activities of ^{226}Ra and ^{228}Ra were determined using a ^{214}Pb (352 keV) and ^{228}Ac (911 keV) peak, respectively.

Some samples were measured using a coaxial-type gamma spectrometer to determine ^{228}Ra activities, and using a RaDeCC system to determine ^{226}Ra activities. Mn-fibers were packed in containers (4 cm diameter, 5 cm length of cylinder type, Teflon material) (Figure 6). Because the geometry of sample determines the counting efficiency, Mn-fibers were compressed flatly inserting small cylinder-type reinforced plastics (3.9 cm diameter, 2.5 cm length) (Figure 6). Thereafter, samples were stored for 3 weeks like a well-type method and measured for 1-3 days (Figure 5). The activities of ^{228}Ra were determined using a ^{228}Ac (911 keV) peak. The activities of ^{226}Ra were determined by an emanation method of RaDeCC system developed by Waska et al. (2008). Mn-fibers were sealed for 3-10 days in a PVC column (7 cm diameter, 13 cm length with an O-ring and two metal ball valves fixed at each end with epoxy) for the ingrowth of ^{222}Rn from ^{226}Ra on the Mn-fibers (Waska et al., 2008). Before each measurement, the system was purged with ambient air for 30 min to reduce the system background (Waska et al., 2008). The air-pump was operated for ~15 min at a flow rate of 6-8 L/min to distribute ^{222}Rn emanated from Mn-fibers evenly over the whole system. Thereafter, the air-pump stopped and the valves were closed, and ^{226}Ra activities were counted for 3-4 hours.

Samples measured by a coaxial-type gamma counter for ^{228}Ra were also measured using a well-type gamma counter for the inter-comparison (Table 1). The

result shows that ^{228}Ra activities from each gamma counter fall within counting error of each other. The propagated errors of ^{228}Ra and ^{226}Ra activities from a well-type gamma counter, ^{228}Ra activities from a coaxial-type gamma counter, and ^{226}Ra activities from the RaDeCC system were 9%, 2%, 9%, and 3%, respectively. Counting efficiencies of a well-type gamma counter for ^{228}Ra and ^{226}Ra, a coaxial-type gamma counter for ^{228}Ra, and the RaDeCC system for ^{226}Ra were 2.8% (n = 5), 7.4% (n = 5), 0.4% (n = 6), and 88% (n = 5), within 2 sigma uncertainties, respectively.

Table 1. The inter-calibration results between a well-type and a coaxial-type gamma counter for ^{228}Ra activity data from the southern sea of Korea.

Sample no.	^{228}Ra activity (dpm/100 L)	
	Well-type	Coaxial-type
S17	33.96 ± 3.15	32.55 ± 2.67
S18	57.23 ± 4.60	56.93 ± 2.49
S19	31.07 ± 2.64	31.33 ± 2.44
S21	16.60 ± 2.46	16.96 ± 1.93
S24	23.22 ± 2.54	23.92 ± 2.31
S30	18.09 ± 2.44	20.14 ± 1.44
S37	22.93 ± 1.89	24.91 ± 2.26
S38	32.84 ± 2.78	33.48 ± 2.58
S39	29.32 ± 2.51	28.24 ± 2.39

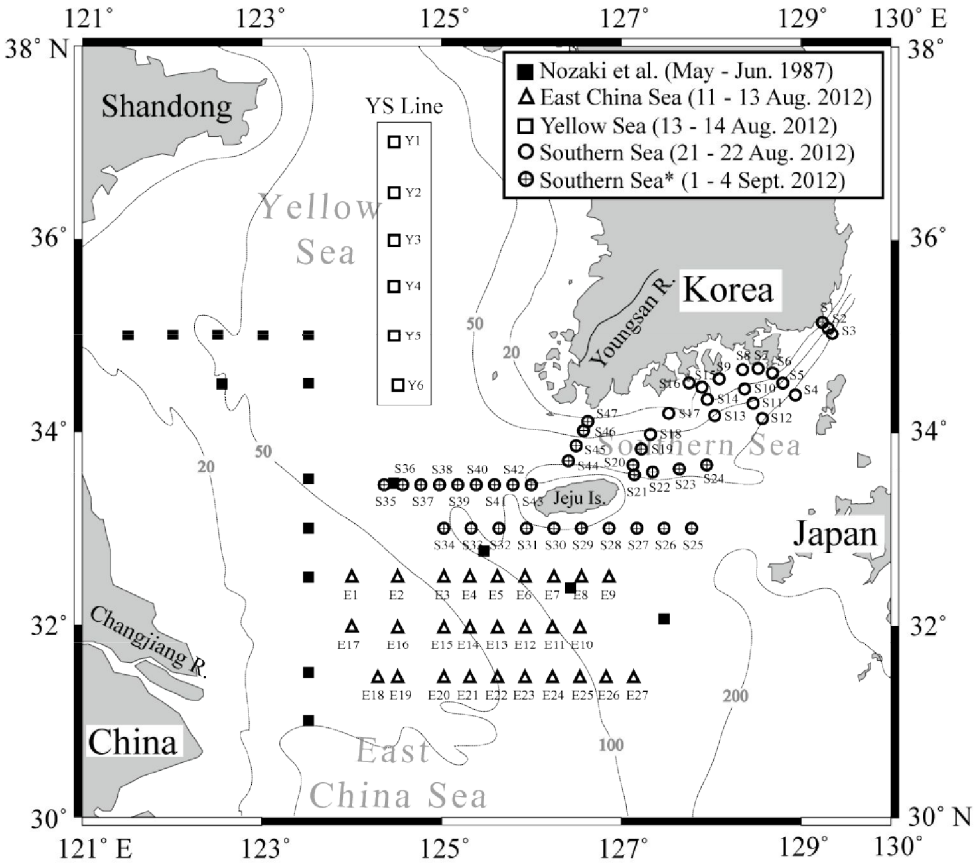

Figure 2. The map of sampling sites in the northwestern Pacific marginal seas including the Yellow Sea, the southern sea of Korea, and the East China Sea during August 11 to September 4, 2012.

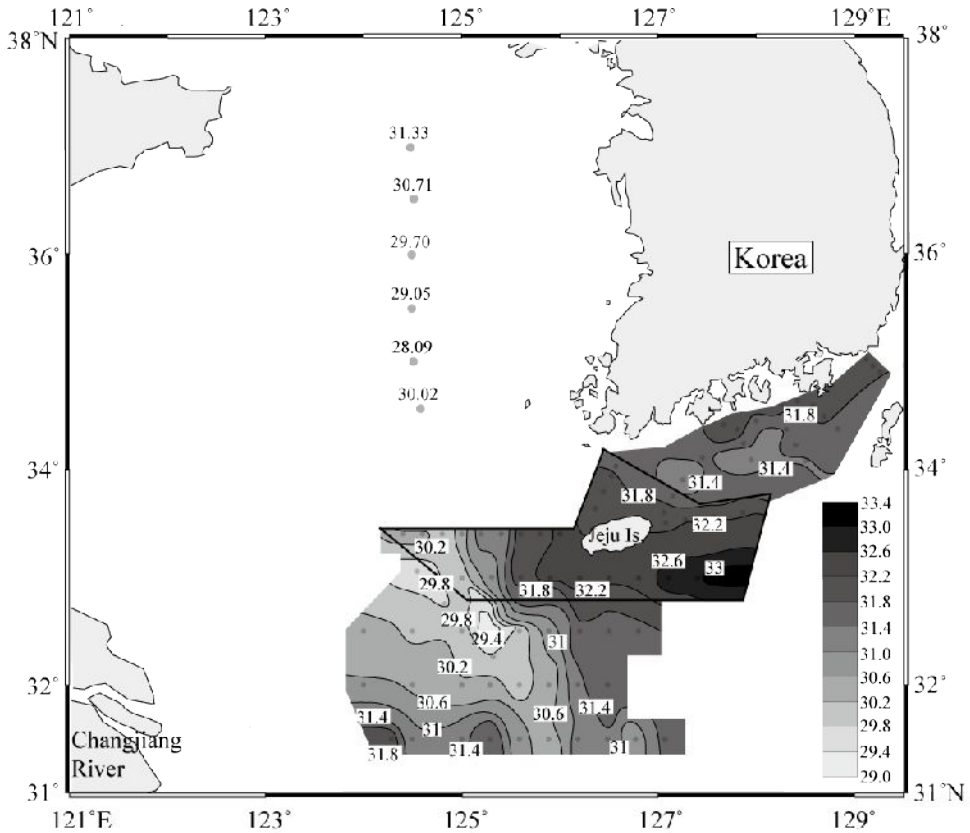

Figure 3. The distribution of salinity in surface seawater of the Yellow Sea, the southern sea of Korea, and the East China Sea during August 11 to September 4, 2012.

Figure 4. The radium delayed coincidence counter (RaDeCC) system used for measuring short-lived ^{223}Ra and ^{224}Ra isotopes.

Figure 5. The inside of a well-type (left side) and a coaxial-type (right side) gamma counter used for measuring ^{226}Ra and ^{228}Ra isotopes.

Figure 6. The container and a small cylinder for compressing a Mn-fiber flatly, which are used for a coaxial-type gamma counter to measure ^{228}Ra activities.

3. Results and Discussion

3.1 Distributions of salinity, temperature, and Ra isotopes

Salinity, temperature, and Ra isotopes data from the East China Sea, the Yellow Sea, and the southern sea of Korea are represented in Table 3, 4, and 5, respectively. The distribution of salinities in surface seawater shows that the low-salinity (<31.4) water is widely distributed over the northern East China Sea, and even to the innermost Yellow Sea (Figure 3). On the contrary, water with relatively higher salinity (>31.4) is observed in the southern sea of Korea and in the northeastern part of the East China Sea. This distribution indicates that surface seawater in the northern East China Sea and the Yellow Sea are considerably influenced by CDW during the summer (Chen et al., 1994). Two patches of low salinity, <29.4 and <29.8, were discovered southwest of Jeju Island. This phenomenon has been often observed between the river mouth and Jeju Island during the summer flooding season (Chen et al., 2008). This seems to be caused by the detachment of anticyclonic eddies as a result of baroclinic instability of the CDW front and subsequent transport toward Jeju Island (Chen et al., 2008).

The distribution of temperatures in surface seawater shows that relatively lower temperatures (<24°C) are discovered in the inner part of the solid line around Jeju Island (Figure 7). This seems to be caused by rigorous vertical mixing, because the survey in this area was conducted approximately 3 days after Typhoon Bolaven. This is also supported by the fact that the vertical gradient of temperatures (not shown here) in the inner part of the solid line was weaker than that of other stations sampled before Typhoon. Salinities of surface seawater in this

area were also somewhat higher than adjacent sea area because of vertical mixing effects (Figure 3).

The distribution of ^{223}Ra ($t_{1/2}$ = 11.4 days) activities in surface seawater shows a good reduction pattern with increasing distance from the mouth of the Changjiang River (Figure 8). This trend seems to be caused by dominant inputs of Ra from the river plume, where extensive Ra desorption occurs from riverine or suspended sediments, and subsequent radioactive decay during the river plume spreads over the shelf (Moore and Krest, 2004). The distribution of ^{224}Ra activities in surface seawater (Figure 9) shows a similar pattern, but these activities maybe originated from local sources such as diffusion from bottom sediments or submarine groundwater discharge (SGD), because ^{224}Ra supplied from the river plume almost decay within ~100 km due to its short half-life ($t_{1/2}$ = 3.6 days) (Moore, 2000).

On the other hand, the activities of long-lived ^{228}Ra ($t_{1/2}$ = 5.75 years) and ^{226}Ra ($t_{1/2}$ = 1,620 years) did not show such a reduction pattern from the river mouth to northeastward (Figure 10 and 11). ^{228}Ra and ^{226}Ra are highly enriched in the Yellow Sea because of continuous benthic input such as SGD and diffusion from shallow bottom sediments (~50 m mean water depth) over a long water residence time (~5 years) (Nozaki et al., 1991; Kim et al., 2005) (Figure 13). High activities of ^{226}Ra at some stations between the river mouth and Jeju Island are presumably due to SGD, because ^{226}Ra is largely influenced by groundwater discharge rather than by diffusion from bottom sediments (Kim et al., 2005) (Figure 11). Kim et al. (2001b) also reported that significant excess Ra activities were detected in surface seawater of the East China Sea shelf area.

Plots of ^{223}Ra and ^{224}Ra activities as a function of salinity show that five

samples in the southern sea of Korea show abnormally high activities in the salinity range between 31 and 32 (Figure 12). These high activities were all discovered at the southwestern part of the southern sea of Korea (Figure 8 and 9). One possibility of this phenomenon is that high activities were originated from the Yellow Sea by Korean Coastal Current (KCC). However, considering that activities of ^{223}Ra and ^{224}Ra in the Yellow Sea were similar to or lower than those in the southwestern part of the southern sea of Korea and theirs half-lives are relatively short in this space scale, this explanation is not persuasive. More plausible reason is that it could be most likely caused by local inputs from diffusion from bottom sediments and the rapid regeneration from suspended sediments because off the southwest tip of the Korean Peninsula generally shows the highest concentration of suspended sediments (Wells, 1988; Hancock and Murray, 1996). The activities of ^{228}Ra also show somewhat high in the southwestern tip of the Korean Peninsula, but long-lived ^{226}Ra activities show no this pattern because the regeneration rates of ^{226}Ra are much lower than other three Ra isotopes (^{223}Ra, ^{224}Ra, and ^{228}Ra) (Hwang et al., 2005) (Figure 9 and 10) .

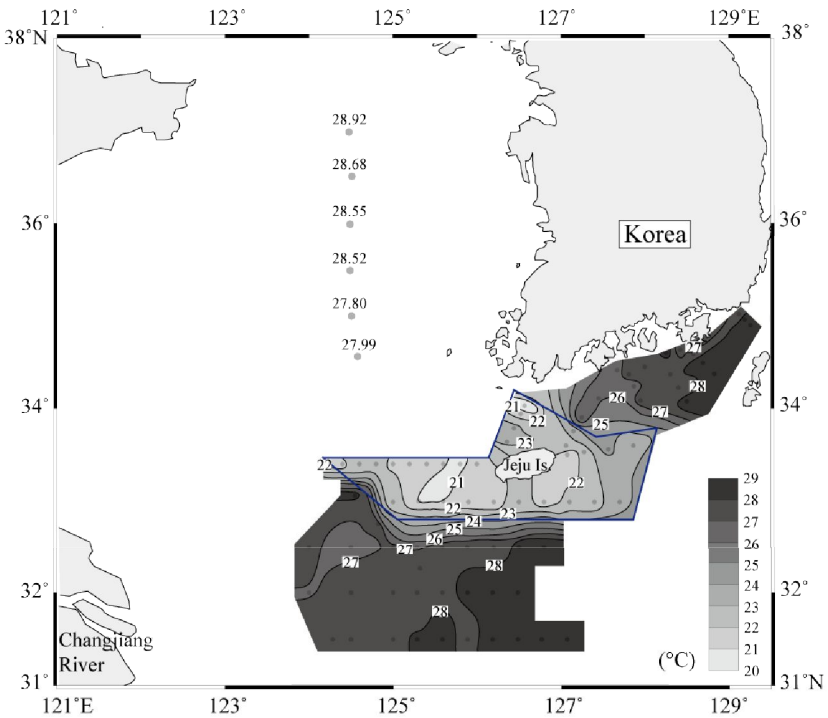

Figure 7. The distribution of temperatures in surface seawater of the Yellow Sea, the southern sea of Korea, and the East China Sea during August 11 to September 4, 2012.

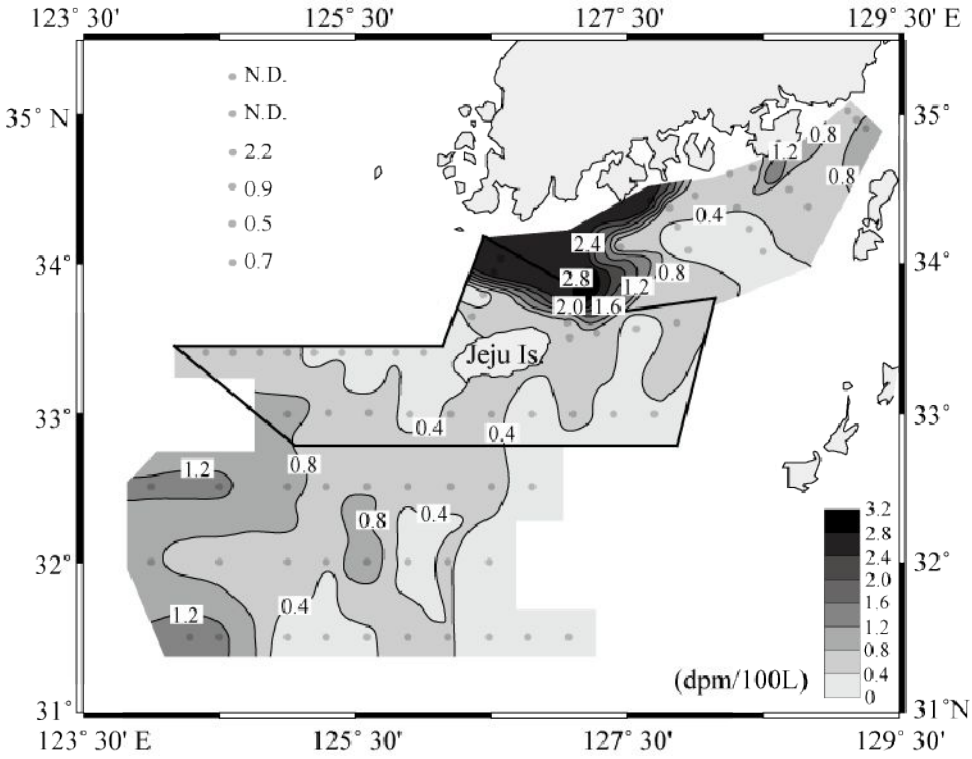

Figure 8. The contour map of ^{223}Ra activities in surface seawater of the Yellow Sea, the southern sea of Korea, and the East China Sea during August 11 to September 4, 2012.

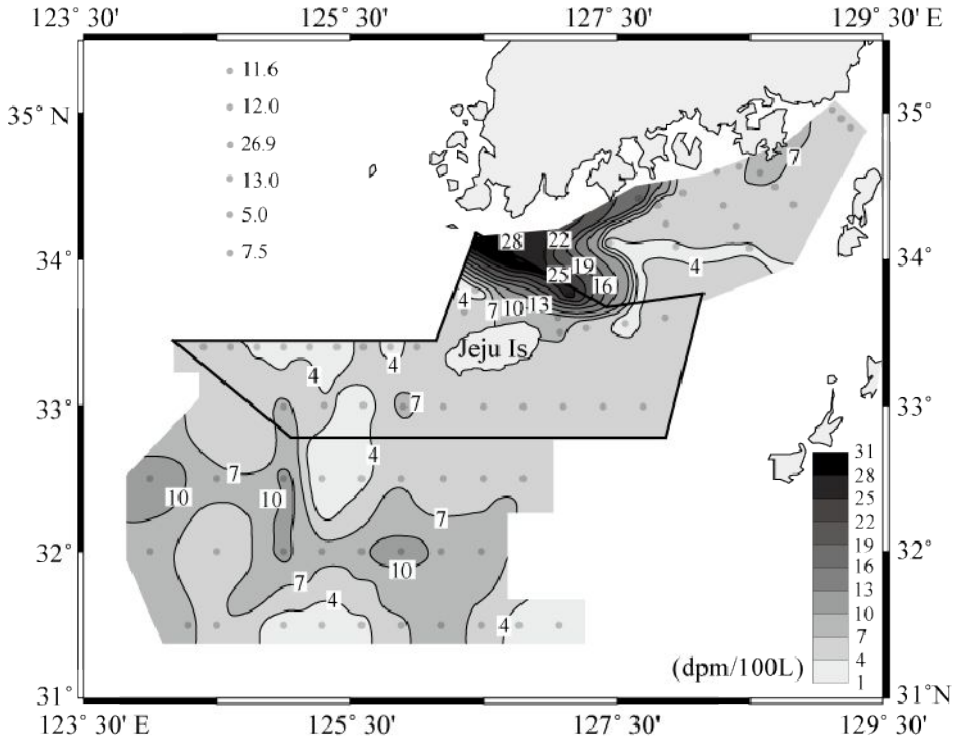

Figure 9. The contour map of ^{224}Ra activities in surface seawater of the Yellow Sea, the southern sea of Korea, and the East China Sea during August 11 to September 4, 2012.

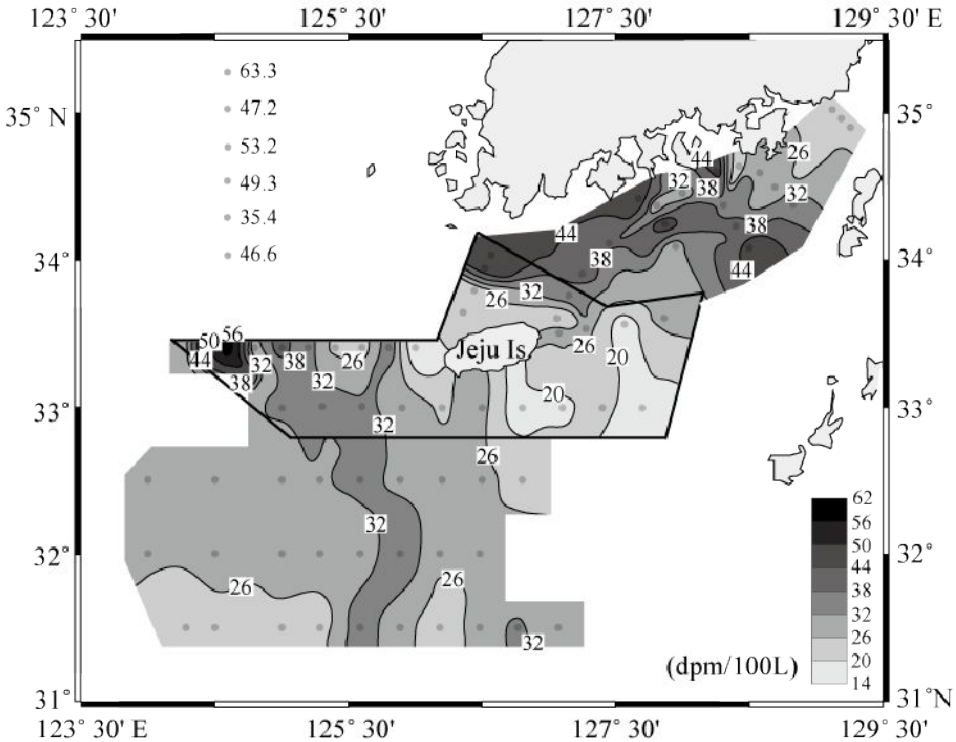

Figure 10. The contour map of ^{228}Ra activities in surface seawater of the Yellow Sea, the southern sea of Korea, and the East China Sea during August 11 to September 4, 2012.

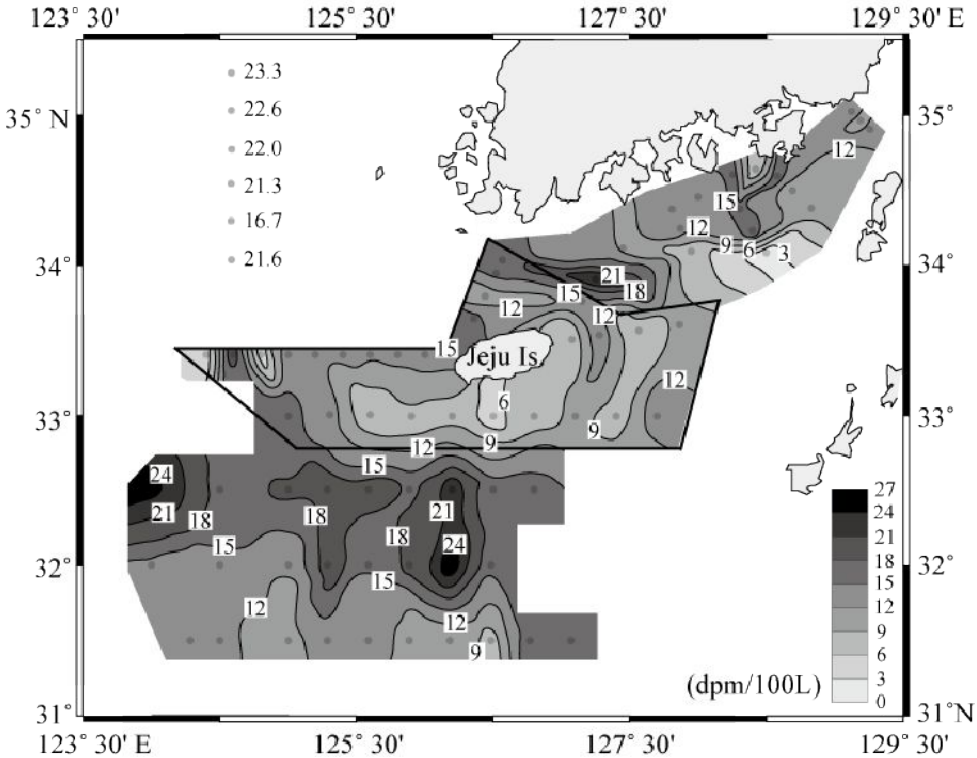

Figure 11. The contour map of ^{226}Ra activities in surface seawater of the Yellow Sea, the southern sea of Korea, and the East China Sea during August 11 to September 4, 2012.

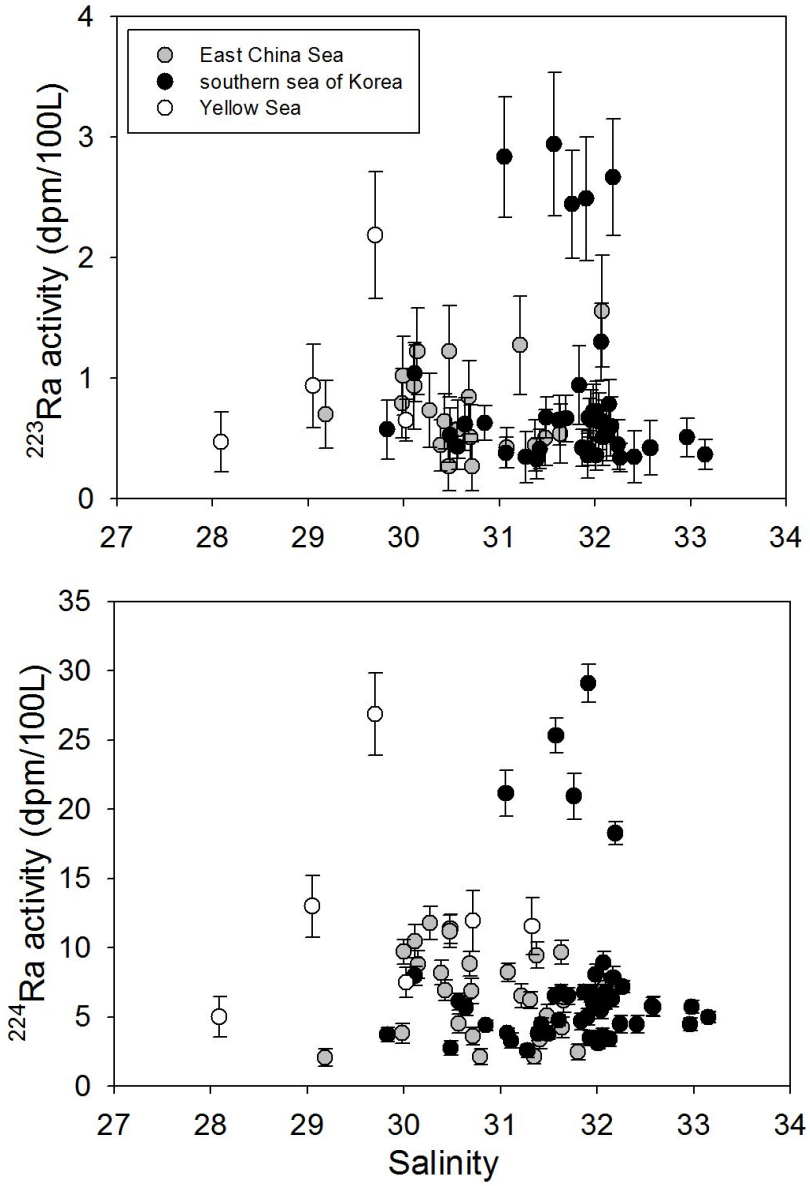

Figure 12. Plots of ^{223}Ra (upper) and ^{224}Ra activities (bottom) as a function of salinity in surface seawater of the Yellow Sea, the southern sea of Korea, and the East China Sea during August 11 to September 4, 2012.

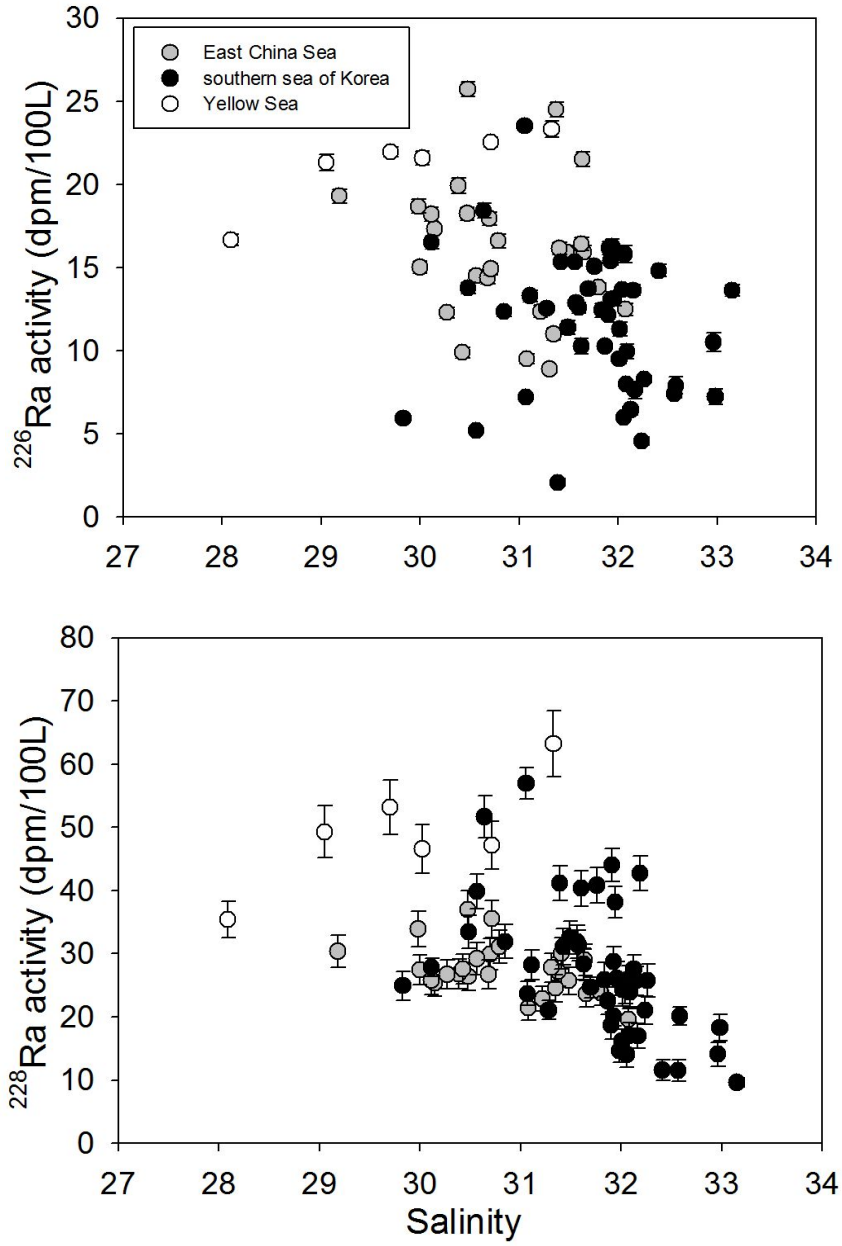

Figure 13. Plots of ^{226}Ra (upper) and ^{228}Ra (bottom) activities as a function of salinity in surface seawater of the Yellow Sea, the southern sea of Korea, and the East China Sea during August 11 to September 4, 2012.

Table 2. Temperature, salinity, and Ra isotopes (^{223}Ra, ^{224}Ra, ^{226}Ra, and ^{228}Ra) data in surface seawater of the East China Sea.

Date	Station	Sal.	Temp. (°C)	^{223}Ra	^{224}Ra	^{226}Ra	^{228}Ra
				dpm/100L			
11 Aug. 2012	E1	30.48	27.16	1.22±0.38	11.36±1.05	25.71±0.44	26.42±2.23
	E2	30.14	26.40	1.22±0.36	8.78±0.99	17.32±0.24	25.36±2.07
	E3	30.11	27.32	0.93±0.36	10.48±1.20	18.21±0.40	25.79±2.20
	E4	29.18	26.99	0.70±0.28	2.04±0.64	19.30±0.41	30.36±2.56
	E5	29.98	27.73	0.79±0.29	3.80±0.71	18.69±0.41	33.91±2.85
	E6	30.70	27.89	0.51±0.27	6.86±0.93	17.96±0.39	29.91±2.53
	E7	31.64	27.57	0.54±0.25	4.22±0.74	21.52±0.44	29.03±2.46
	E8	31.48	28.25	0.51±0.23	5.10±0.78	15.95±0.37	25.68±2.19
	E9	31.65	28.45	N.D	6.20±0.88	15.94±0.39	23.67±2.04
12 Aug. 2012	E10	31.63	28.35	N.D	9.66±0.88	16.43±0.38	28.32±2.40
	E11	31.38	28.42	0.44±0.21	9.45±0.95	24.50±0.44	27.17±2.29

* N.D : non detectable

Continued.

Date	Station	Sal.	Temp. (°C)	^{223}Ra	^{224}Ra	^{226}Ra	^{228}Ra
				dpm/100L			
12 Aug. 2012	E12	30.47	28.13	0.27±0.20	11.18±1.18	18.25±0.40	36.98±3.10
	E13	29.99	27.77	1.02±0.33	9.69±0.88	15.03±0.38	27.40±2.35
	E14	30.38	27.66	0.44±0.21	8.18±0.88	19.92±0.45	26.79±2.31
	E15	30.27	27.85	0.73±0.31	11.78±1.23	12.29±0.42	26.72±2.27
	E16	30.57	27.96	0.57±0.24	4.51±0.70	14.51±0.36	29.21±2.48
	E17	30.68	26.99	0.84±0.30	8.83±0.86	14.38±0.34	26.69±2.26
	E18	32.08	27.52	1.56±0.46	7.11±0.91	12.48±0.37	19.54±1.74
	E19	31.21	27.58	1.27±0.41	6.53±0.85	12.35±0.37	22.85±2.00
13 Aug. 2012	E20	31.34	27.70	N.D	2.14±0.53	10.99±0.36	24.51±2.16
	E21	31.80	28.06	N.D	2.44±0.57	13.83±0.24	23.77±1.96
	E22	30.71	28.27	0.27±0.20	3.60±0.63	14.92±0.34	35.53±2.96
	E23	30.43	27.84	0.64±0.23	6.90±0.75	9.88±0.31	27.57±2.37

Continued.

Date	Station	Sal.	Temp. (°C)	^{223}Ra	^{224}Ra	^{226}Ra	^{228}Ra
				dpm/100L			
13 Aug. 2012	E24	31.08	28.37	0.42±0.17	8.21±0.66	9.52±0.29	21.38±1.85
	E25	31.31	28.06	N.D	6.21±0.63	8.89±0.20	27.81±2.29
	E26	30.79	28.26	N.D	2.11±0.58	16.60±0.40	31.12±2.64
	E27	31.41	28.49	N.D	3.35±0.68	16.15±0.38	30.06±2.55

Table 3. Temperature, salinity, and Ra isotopes (^{223}Ra, ^{224}Ra, ^{226}Ra and ^{228}Ra) data in surface seawater of the Yellow Sea.

Date	Station	Sal.	Temp. (°C)	^{223}Ra	^{224}Ra	^{226}Ra	^{228}Ra
				dpm/100L			
13 Aug. 2012	Y1	31.33	28.92	N.D	11.55±2.05	23.32±0.47	63.26±5.21
	Y2	30.71	28.68	N.D	11.93±2.21	22.55±0.31	47.16±3.83
	Y3	29.70	28.55	2.19±0.52	26.88±2.95	21.97±0.30	53.19±4.31
14 Aug.2012	Y4	29.05	28.52	0.94±0.35	12.99±2.24	21.31±0.49	49.29±4.13
	Y5	28.09	27.80	0.47±0.25	5.00±1.44	16.67±0.34	35.43±2.94
	Y6	30.02	27.99	0.65±0.18	7.48±1.10	21.59±0.43	46.60±3.86

Table 4. Temperature, salinity, and Ra isotopes (^{223}Ra, ^{224}Ra, ^{226}Ra, and ^{228}Ra) data in surface seawater of the southern sea of Korea.

Date	Station	Sal.	Temp. (°C)	^{223}Ra	^{224}Ra	^{226}Ra	^{228}Ra
				dpm/100L			
21 Aug. 2012	S1	31.96	27.77	0.65±0.25	6.03±0.57	13.12±0.44	26.07±2.72
	S2	32.02	28.09	0.73±0.25	5.79±0.61	11.29±0.42	24.33±2.56
	S3	31.83	28.48	0.94±0.33	4.67±0.59	12.42±0.43	25.91±2.70
	S4	31.63	28.35	0.65±0.20	6.81±0.49	10.26±0.48	28.36±2.53
	S5	31.86	28.85	0.42±0.15	6.77±0.56	10.26±0.18	22.55±2.14
	S6	32.07	27.13	1.30±0.32	8.91±0.81	15.80±0.51	25.85±2.19
	S7	32.08	26.56	0.64±0.17	5.97±0.40	7.97±0.17	17.03±2.01
	S8	31.94	28.03	0.67±0.16	6.71±0.50	16.25±0.49	38.15±2.53
	S9	31.70	27.71	0.67±0.19	6.50±0.59	13.73±0.34	24.67±1.66
	S10	31.42	27.78	0.41±0.16	4.46±0.43	15.33±0.23	31.08±2.84
	S11	31.56	27.47	N.D	6.52±0.56	15.35±0.25	31.93±2.64

Continued. (‘-’ denotes ‘not measured’)

Date	Station	Sal.	Temp. (°C)	^{223}Ra	^{224}Ra	^{226}Ra	^{228}Ra
				dpm/100L			
21 Aug. 2012	S12	31.39	28.24	0.33±0.17	3.80±0.46	2.07±0.21	41.18±2.79
22 Aug. 2012	S13	31.07	27.25	0.38±0.13	3.83±0.34	7.21±0.15	23.67±1.88
	S14	31.60	26.47	N.D	4.76±0.40	12.58±0.31	40.39±2.82
	S15	32.15	27.41	0.78±0.20	6.29±0.57	13.64±0.32	25.68±2.30
	S16	32.19	26.91	2.67±0.48	18.27±0.82	-	42.73±2.75
	S17	31.49	26.02	0.68±0.17	3.78±0.38	11.39±0.42	32.55±2.67
	S18	31.05	26.34	2.84±0.50	21.18±1.65	23.53±0.24	56.93±2.49
1 Sept.	S19	31.57	23.15	2.94±0.59	25.32±1.25	12.86±0.34	31.33±2.44
	S20	31.98	22.75	0.72±0.23	8.04±0.74	-	14.62±1.79
	S21	32.17	21.59	0.60±0.25	7.83±0.83	7.63±0.53	16.96±1.93
	S22	32.04	22.23	0.64±0.24	5.47±0.60	13.66±0.22	24.22±2.07
	S23	32.05	24.12	N.D	3.67±0.53	5.98±0.22	14.02±2.04

Continued.

Date	Station	Sal.	Temp. (°C)	^{223}Ra	^{224}Ra	^{226}Ra	^{228}Ra
				dpm/100L			
1 Sept. 2012	S24	32.09	22.97	0.51±0.24	6.81±0.78	9.94±0.44	23.92±2.31
2 Sept. 2012	S25	33.15	23.89	0.37±0.12	4.96±0.40	13.63±0.35	9.58±0.75
	S26	32.98	22.69	N.D	5.71±0.46	7.23±0.45	18.27±2.07
	S27	32.96	22.11	0.51±0.16	4.46±0.46	10.51±0.58	14.07±1.89
	S28	32.57	21.74	N.D	5.75±0.68	7.40±0.23	11.51±1.70
	S29	32.24	22.70	0.45±0.21	4.48±0.63	4.55±0.25	21.00±2.20
3 Sept. 2012	S30	32.58	21.36	0.42±0.23	5.74±0.69	7.91±0.50	20.14±1.44
	S31	32.26	21.58	0.34±0.12	7.18±0.44	8.27±0.18	25.73±2.62
	S32	32.13	21.00	0.54±0.22	3.40±0.52	6.44±0.29	27.51±2.32
	S33	30.85	21.01	0.63±0.14	4.38±0.38	12.34±0.27	31.89±2.68
	S34	30.11	22.79	1.04±0.23	7.97±0.69	16.54±0.38	27.82±1.45
	S35	30.56	21.96	0.43±0.19	6.10±0.60	5.19±0.25	39.86±2.74

Continued.

Date	Station	Sal.	Temp. (°C)	^{223}Ra	^{224}Ra	^{226}Ra	^{228}Ra
				dpm/100L			
3 Sept. 2012	S36	30.64	22.34	0.62±0.22	5.69±0.62	18.43±0.42	51.69±3.39
	S37	29.83	22.69	0.57±0.24	3.72±0.53	5.92±0.14	24.91±2.26
	S38	30.48	21.90	0.53±0.23	2.74±0.51	13.77±0.35	33.48±2.58
	S39	31.11	21.81	N.D	3.27±0.53	13.30±0.36	28.24±2.39
	S40	31.28	21.74	0.35±0.21	2.56±0.49	12.53±0.22	21.07±1.48
4 Sept. 2012	S41	31.90	21.05	N.D	5.00±0.62	12.13±0.13	18.66±2.18
	S42	31.92	20.85	0.36±0.19	3.48±0.55	13.07±0.26	28.77±2.32
	S43	32.41	21.69	0.35±0.22	4.47±0.64	14.82±0.37	11.56±1.68
	S44	31.93	23.83	0.42±0.14	6.56±0.48	15.42±0.28	20.14±1.55
	S45	32.01	23.20	0.36±0.12	3.07±0.37	9.52±0.29	16.18±1.90
	S46	31.76	21.57	2.44±0.45	20.95±1.65	15.07±0.24	40.86±2.82
	S47	31.91	20.51	2.49±0.51	29.10±1.35	16.18±0.39	44.07±2.65

3.2 Flow rate of Changjiang diluted water (CDW)

As mentioned earlier, the northern East China Sea has the distinct feature that a large amount of CDW moves toward Jeju Island in the summer. The timescale of mixing processes between river water and coastal seawater is generally on the order of days to weeks (Moore et al., 2004). Thus, in this study, ^{223}Ra was used to estimate the flow rate of CDW from the river mouth to northeastward because its half-life ($t_{1/2}$ = 11.4 days) is suitable for this timescale, and high sediment loading during the summer flooding season can be a strong source of ^{223}Ra (Milliman et al., 1985). The plot of ^{223}Ra activities versus distances from the river mouth, showing a good exponential decay pattern, demonstrates that ^{223}Ra is a suitable tracer of the flow rate of CDW in this space scales (~ 500 km) (Figure 14).

Assuming that (1) ^{223}Ra in surface seawater of the northern East China Sea is supplied predominantly from the Changjiang River plume and (2) the surface layer is separate from the subsurface layer during the summer flooding season (Chu et al., 2005), the flow rate of CDW can be calculated using following equations.

$$^{223}Ra_{obs} = {}^{223}Ra_i \times e^{-0.0045 \times d} \quad (1)$$

$$^{223}Ra_{obs} = {}^{223}Ra_i \times e^{-\lambda 223 \times t} = {}^{223}Ra_i \times e^{-\lambda 223 \times (d/v)} \quad (2)$$

where Ra_i is the initial activity of ^{223}Ra at the river mouth (0 km), Ra_{obs} is ^{223}Ra

activity at the distance from the river mouth, λ_{223} is the decay constant of ^{223}Ra (λ_{223} = 0.0608/d), d is the distance (km) from the river mouth, t is the arrival time from the river mouth to the observed point, and v is the current speed (km/d) of the CDW.

In order to obtain an initial activity of ^{223}Ra at the river mouth (0 km), ^{223}Ra data from this study were extrapolated to the river mouth (Figure 14). The extrapolated value was 3.1 ± 0.2 dpm/100 L, which agreed very well with the ^{223}Ra activity (3.2 ± 0.4 dpm/100 L) from Gu et al. (2012) at the river mouth, within counting uncertainties. This agreement suggests that the activities of ^{223}Ra in this region are very consistent in summer for different years. Thus, this extrapolated value is used here as an initial ^{223}Ra activity for estimating the flow rate of CDW.

Using the regression equation (1) of Figure 11, the activity of ^{223}Ra (0.42 dpm/100 L) was obtained at a distance (~450 km) from the river mouth to the vicinity of Jeju Island. Substituting this value to equation (2), current speed of the CDW from the river mouth to the vicinity of Jeju Island was determined. This function provided good estimates of statistical significance ($p<0.0001$, $r^2 = 0.89$).

The result shows that the arrival time and current speed of CDW from the river mouth to the vicinity of Jeju Island were estimated to be 33 ± 2 days and 16 ± 1 cm/s, respectively. These results are comparable to previous studies that used physical methods such as surface drifter buoys and numerical modeling (Lie et al., 2003; Chen et al., 2008; Moon et al., 2009). Although current speeds are variable according to the wind strength, Moon et al. (2009) revealed that surface particles released at the river mouth are transported to Jeju Island in 45–50 days using a three-dimensional model. Lie et al. (2003) reported that the mean speeds of

satellite-tracked drifters from river mouth eastward toward Jeju Island were 11–12 cm/s in June–July 1997 and 22–28 cm/s in July–August 1998 respectively, during which heavy flooding occurred upstream of the Changjiang River. The mean speed from the river mouth to Jeju Island in the warm half of the year was determined to be 21.2 cm/s using surface drifters (Ichikawa and Beardsley, 2002). Considering that the mean current speeds from physical studies were obtained by only a few buoys, this estimation (16 ± 1 cm/s) is more representative of current speed of CDW from the river mouth to northeastward toward the vicinity of Jeju Island because large area was integrated in this estimation.

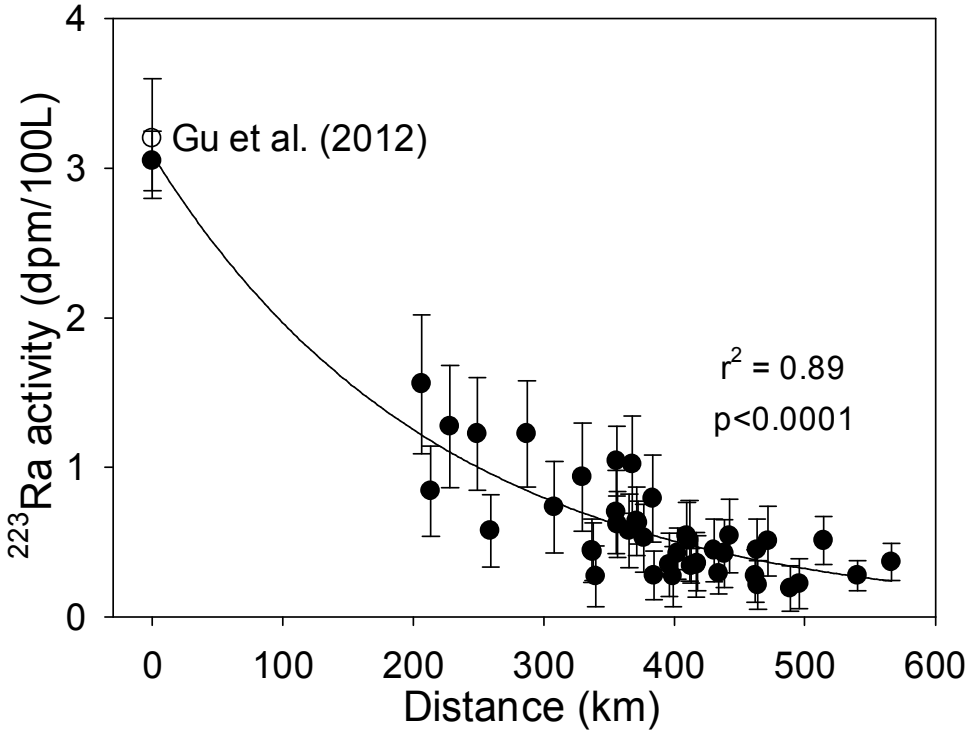

Figure 14. Plot of ^{223}Ra activities as a function of distances from the mouth of the Changjiang River (0 km).

3.3 Mixing proportion of Changjiang diluted water (CDW)

In general, CDW is mixed into (1) Kuroshio water and (2) the Yellow Sea water in the northern East China Sea, the southern sea of Korea, and the Yellow Sea (Kim and Han, 2000). The Kuroshio water, which flows northward through the East China Sea all year has almost constant salinity over 34.7, and the proper water of the Yellow Sea has salinity between 31 and 32 because of a strong winter mixing over a water residence time of ~5 years (Nozaki et al., 1991; Kim et al., 2001b). As mentioned earlier, the salinity of CDW is lower than 32. Therefore, it is extremely difficult to determine the relative contribution of CDW in this region. However, it can be differentiated using a ^{228}Ra-salinity diagram because each water mass have different ^{228}Ra activities (Figure 15).

The end-member values of each water mass are from Nozaki et al. (1991) for the Yellow Sea water and the Kuroshio water and from Gu et al. (2012) for the CDW. The end-member of CDW is obtained from the average of four surface water samples, which have salinities from 27 to 28, in front of the river mouth between 30.5°N and 31.5°N, 122.5°E and 123°E to avoid significant Ra desorption effects on riverine fresh sediments (Webster et al., 1995). The end-member of the Kuroshio water was obtained from the average of six samples in surface water of the Kuroshio Current (Nozaki et al., 1991). In case of the Yellow Sea water, it is defined here as the water which shows highest ^{228}Ra (73 dpm/100 L) activity in the central part of the Yellow Sea. If we assume that the end-member of ^{228}Ra is 1.7, 73, and 36 dpm/100 L and the end-member of salinity is 34.7, 31.5, and 27.8 for Kuroshio water, Yellow Sea water, and CDW, respectively, the relative

contributions of CDW can be calculated using following equations (3-5).

$$f \cdot S_y + g \cdot S_c + h \cdot S_k = S_m \quad (3)$$

$$f \cdot Ra_y + g \cdot Ra_c + h \cdot Ra_k = Ra_m \quad (4)$$

$$f + g + h = 1 \quad (5)$$

where S_y, S_c, and S_k are the end-members of salinity; Ra_y, Ra_c, and Ra_k are the end-members of ^{228}Ra activity; f, g, and h are the mixing proportions of the Yellow Sea water, CDW, and Kuroshio water, respectively; and S_m and Ra_m are the measured salinities and ^{228}Ra activities. In this approach, ^{226}Ra is not used as part of a pair because it is largely influenced by groundwater discharge rather than diffusion from bottom sediments (Kim et al., 2005).

The calculated relative contributions of the CDW in surface water of the YS line, the northern East China Sea, and the southern sea of Korea are shown in Figure 16 and 17. The contribution of the CDW in surface water of the northern East China Sea and the YS line was more than 50% in most of the sampling stations, indicating dominant contributions of the CDW in this region during the summer flooding season. The surface water of the YS line was dominantly composed of the Yellow Sea water and the CDW, more than 90% of the total, with a very small contribution from the Kuroshio water. Furthermore, the CDW contributes approximately 30% even between Jeju Strait and Korea/Tsushima Strait. This indicates rapid and significant contributions of the CDW to farther remote regions (Figure 17). The contributions of the Yellow Sea water were almost similar to those of CDW in surface water of the YS line but decreased sharply toward the

East China Sea (Figure 18). However, the contributions of the Yellow Sea water was considerable (30–50%) in surface water of the southern sea of Korea, indicating the importance of the Yellow Sea water in surface water of this region. The contribution of the Kuroshio water was highest (up to 65%) in surface water of the region surrounding Jeju Island (Figure 19).

In this estimation, there are large uncertainties because the end-members of salinity and ^{228}Ra are variable over different spaces and times. Also, the effects of Taiwan Warm Current (TWC) on the study area was not considered because of shortage of Ra data. Although this study is restricted only to the surface layer (<3m), these results indicate that the geochemistry and biology of the northwestern Pacific marginal seas could be influenced significantly by the CDW during the summer flooding season because the CDW is known to have unique biogeochemical characters (i.e., high nutrients and suspended solids).

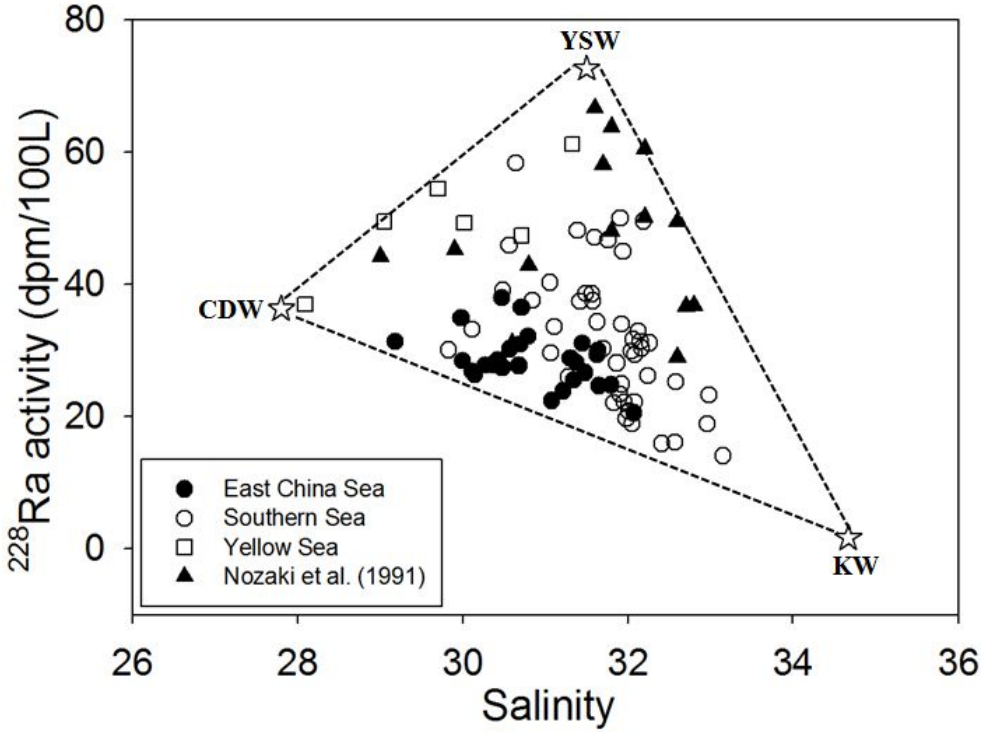

Figure 15. A mixing diagram between ^{228}Ra activity and salinity in surface seawater of the Yellow Sea, the southern sea of Korea, and the East China Sea during August 11 to September 4, 2012.

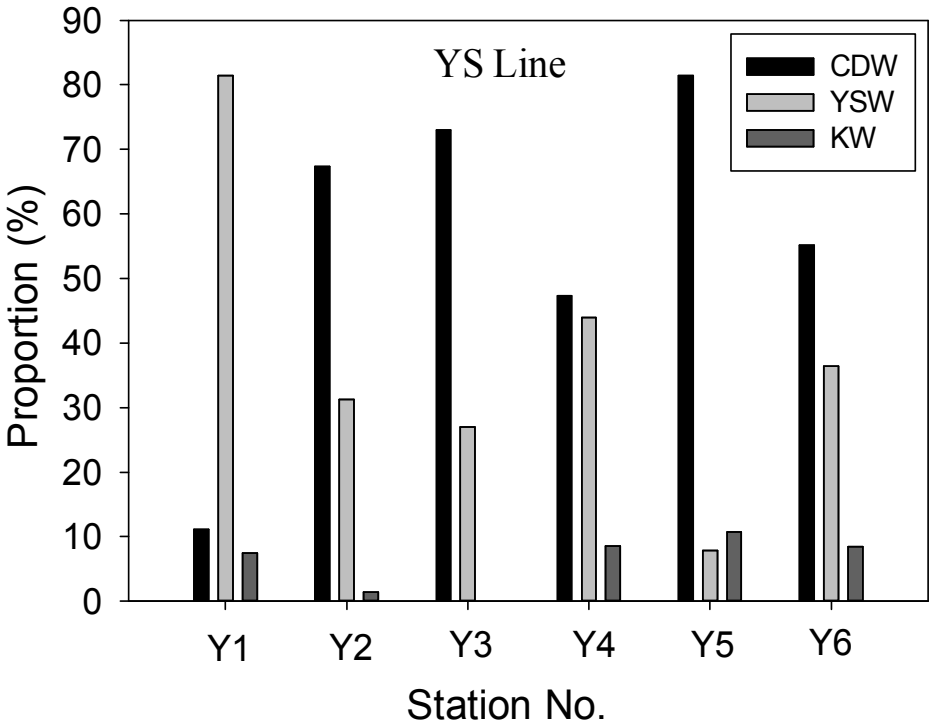

Figure 16. The histogram of the mixing proportions of three end-members, Yellow Sea water (YSW), CDW, and Kuroshio water (KW) at the YS line during August 13 to 14, 2012.

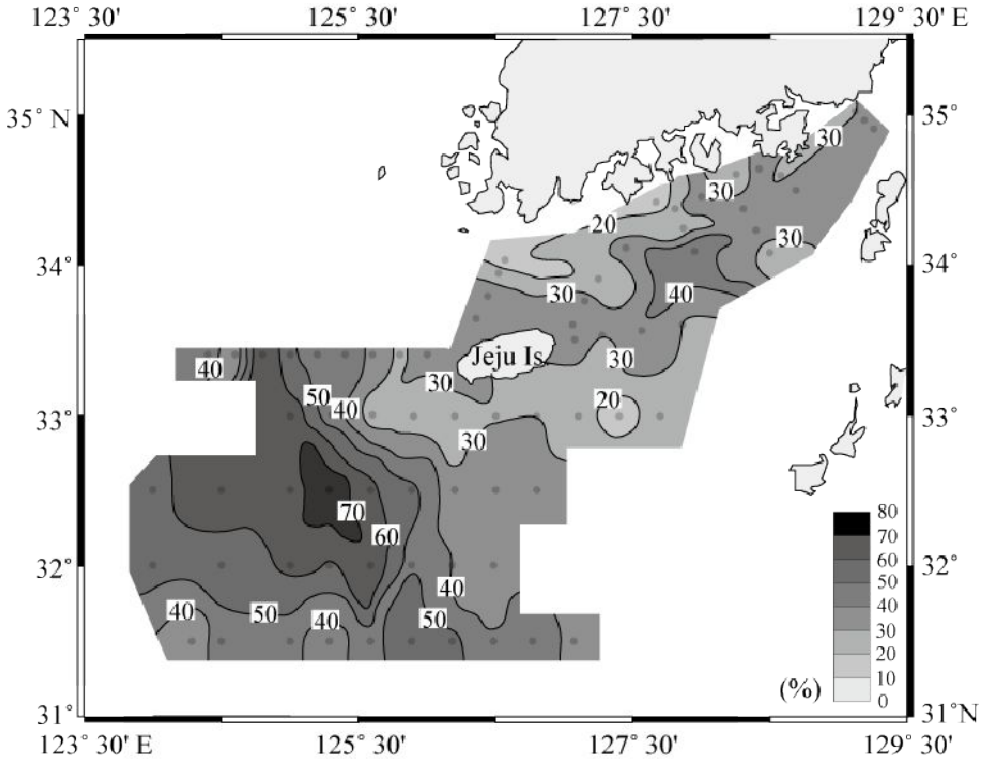

Figure 17. The contour map of mixing proportions of CDW in the southern sea of Korea and the East China Sea during August 11 to September 4, 2012.

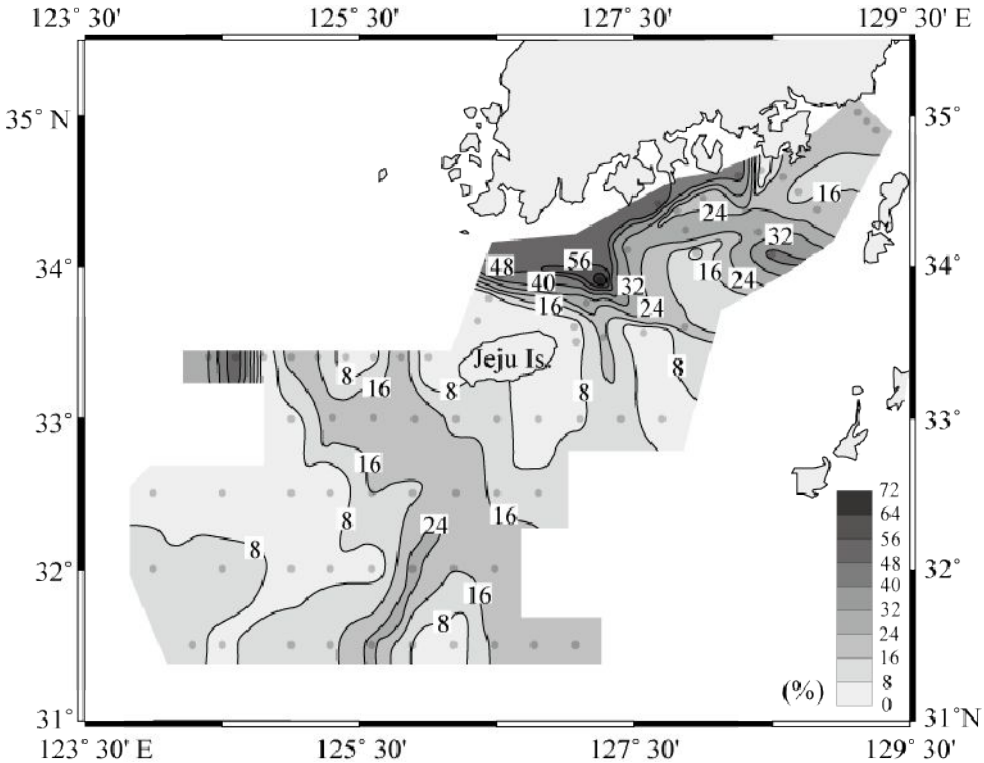

Figure 18. The contour map of mixing proportions of the Yellow Sea water in the southern sea of Korea and the East China Sea during August 11 to September 4, 2012.

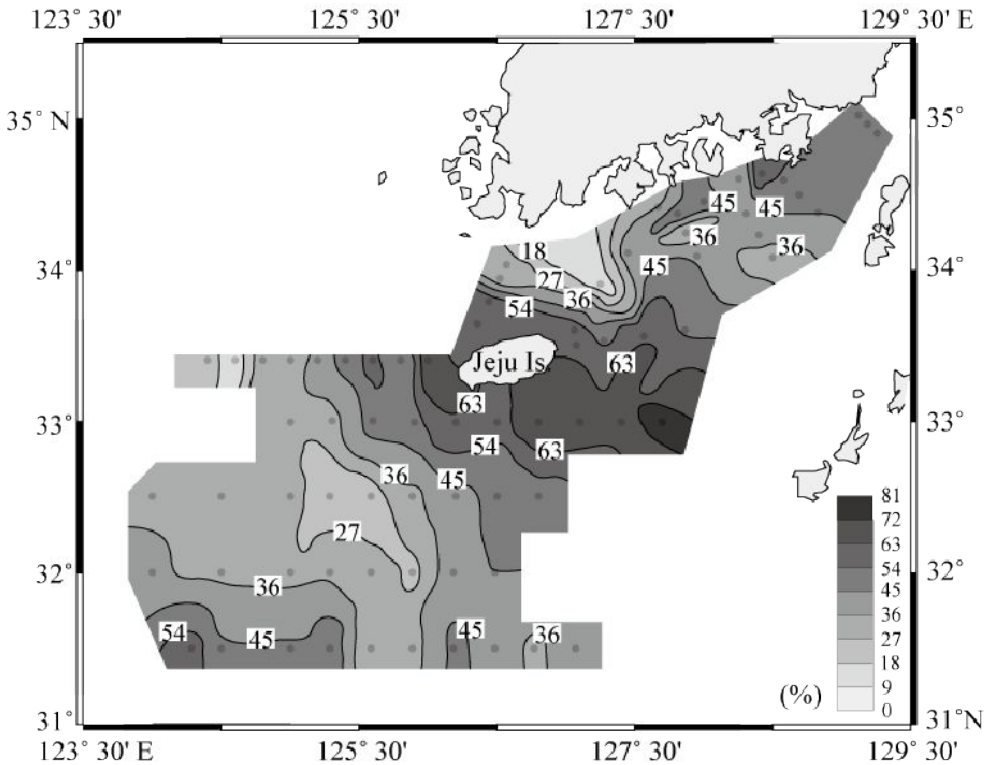

Figure 19. The contour map of mixing proportions of the Kuroshio water in the southern sea of Korea and the East China Sea during August 11 to September 4, 2012.

4. Summary

The flow rate of the CDW in the northern East China Sea was estimated using the decay of ^{223}Ra to be 16 ± 1 cm/s from the river mouth northeastward toward the vicinity of Jeju Island. This result are comparable with the previous studies using physical methods such as surface drifter buoy and numerical modeling. This indicates that the ^{223}Ra method for estimating current speeds of river plume is an excellent alternative to other expensive and time-consuming methods. On the other hand, the relative contributions of the CDW in surface water of the northwestern Pacific marginal seas were successfully calculated using a salinity and ^{228}Ra diagram. During this summer flooding season, the contribution of CDW was more than 50% in surface water of the northern East China Sea and the YS line, and even about 30% to the Korea/Tsushima Strait, which is approximately 800 km from the river mouth. In addition, surface water of the Yellow Sea was composed predominantly of the Yellow Sea water and the CDW. Although this study is restricted only to the surface layer (<3m), these results indicate that the geochemistry and biology of the northwestern Pacific marginal seas could be influenced significantly by the CDW during the summer flooding periods.

5. References

Chang, P. H., and A. Isobe (2003), A numerical study on the Changjiang diluted water in the Yellow and East China Seas, J. Geophys. Res., 108, 3299.

Charette, M. A., K. O. Buesseler, and J. E. Andrews (2001), Utility of Radium Isotopes for Evaluating the Input and Transport of Groundwater-Derived Nitrogen to a Cape Cod Estuary, Limnol. Oceanogr., 46(2), 465-470.

Chen, C., R. C. Beardsley, R. Limeburner, and K. Kim (1994), Comparison of winter and summer hydrographic observations in the Yellow and East China Seas and adjacent Kuroshio during 1986, Cont. Shelf Res., 14, 909-929.

Chen, C., P. Xue, P. Ding, R. C. Beardsley, Q. Xu, X. Mao, G. Gao, J. Qi, C. Li, H. Lin, G. Cowles, and M. Shi (2008), Physical mechanisms for the offshore detachment of the Changjiang Diluted Water in the East China Sea, J. Geophys. Res., 113, JC003994.

Chen, J., F. Wang, X. Xia, and L. Zhang (2002), Major element chemistry of the Changjiang (Yangtze River), Chem. Geol., 187, 231-255.

Cho, Y.-K., G. H. Seo, B.-J. Choi, S. Kim, Y. Kim, and E. P. Dever (2009), Connectivity among straits of the Northwest Pacific Marginal Seas, J. Geophys. Res., 114, JC005218

Chu, P., C. Yuchun, and A. Kuninaka (2005), Seasonal variability of the Yellow Sea/East China Sea surface fluxes and thermohaline structure, Adv. Atmos. Sci., 22, 1-20.

Dulaiova, H. and W. C. Burnett (2004), An efficient method for γ–spectrometric determination of radium-226,228 via manganese fibers, Limnol. Oceanogr.,

Methods 2, 256-261.

Edmond, J. M., A. Spivack, B. C. Grant, H. Ming-hui, and C. Zexiam (1985), Chemical dynamics of the Changjiang estuary, Cont. Shelf Res., 4, 17-36.

Elsinger, R. J. and W. S. Moore (1980), ^{226}Ra behavior in the Pee Dee River-Winyah Bay estuary, Earth Planet. Sci. Lett., 48, 239-249.

Elsinger, R. J. and W. S. Moore (1984), ^{226}Ra and ^{228}Ra in the mixing zones of the Pee Dee River-Winyah bay, Yangtze River and Delaware bay estuaries, Estuar. Coast. Shelf Sci., 18, 601-613.

Garcia-Solsona E., J. Garcia-Orellana, P. Masque, and H. Dulaiova (2008), Uncertainties associated with ^{223}Ra and ^{224}Ra measurements in water via a Delayed Coincidence Counter (RaDeCC), Mar. Chem., 109, 198-219.

Giffin, C., A. Kaufman, and W. Broecker (1963), Delayed Coincidence Counter for the Assay of Actinon and Thoron, J. Geophys. Res., 68, 1749-1757.

Gu, H., W. S. Moore, L. Zhang, J. Du, and J. Zhang (2012), Using radium isotopes to estimate the residence time and the contribution of submarine groundwater discharge (SGD) in the Changjiang effluent plume, East China Sea, Cont. Shelf Res., 35, 95-107.

Hancock, G. J. and A. S. Murray (1996), Source and distribution of dissolved radium in the Bega River estuary, Southeastern Australia, Earth Planet. Sci. Lett., 138, 145-155.

Hwang, D.-W., G. Kim, Y.-W. Lee, H.-S. Yang (2005), Estimating submarine inputs of groundwater and nutrients to a coastal bay using radium isotopes, Mar. Chem., 96, 61-71.

Ichikawa, H. and R. C. Beardsley (2002), The Current System in the Yellow and

East China Seas, J. Oceanogr., 58, 77-92.

Kim, G., W. C. Burnett, H. Dulaiova, P. W. Swarzenski, and W. S. Moore (2001a), Measurements of ^{224}Ra and ^{226}Ra activities in natural waters using a radon-in-air monitor, Environ. Sci. Technol., 35, 4680-4683.

Kim, G. B., H. S. Yang, K. R. Kim, and K. Kim (2001b), Radium isotopes in the Pacific-Asian marginal seas as a water-mass tracer, Extended Abstract Volume, The 11th PAMS/JECSS Workshop, April 11-13, 2001, Cheju, Korea, 397-400.

Kim G, N. Hussain, and T. M. Church (2003), Tracing the advection of organic carbon into the subsurface Sargasso Sea using a ^{228}Ra/^{226}Ra tracer, Geophy. Res. Lett., 30: doi:10.1029/2003GL017565.

Kim, G., J.-W. Ryu, H.-S. Yang, and S.-T. Yun (2005), Submarine groundwater discharge (SGD) into the Yellow Sea revealed by ^{228}Ra and ^{226}Ra isotopes: Implications for global silicate fluxes, Earth Planet. Sci. Lett., 237, 156-166.

Kim, H.-C., H. Yamaguchi, S. Yoo, J. Zhu, K. Okamura, Y. Kiyomoto, K. Tanaka, S.-W. Kim, T. Park, I. S. Oh, and J. Ishizaka (2009), Distribution of Changjiang Diluted Water Detected by Satellite Chlorophyll-a and Its Interannual Variation during 1998-2007, J. Oceanogr., 65, 129-135.

Kim, K. H. and J. H. Han (2000), Origin and mixing ratio of water masses in the East China Sea, the South Sea and the Korea Strait using radium isotopes and salinity, J. Kor. Soc. Oceanogr., 5, 216-223.

Kim, S.-K., K.-I. Chang, B. Kim, and Y.-K. Cho (2013), Contribution of ocean current to the increase in N abundance in the Northwestern Pacific marginal seas, Geophy. Res. Lett., 40, 143-148.

Li, Y.-H., G. Mathieu, P. Biscaye, and H. J. Simpson (1977), The flux of ^{226}Ra from estuarine and continental shelf sediments, Earth Planet. Sci. Lett., 37, 237-241.

Lie, H.-J. (1984), A note on water masses and general circulation in the Yellow Sea (Hwanghae), J. Oceanol. Soc. Korea, 19, 187-194.

Lie, H.-J., C.-H. Cho, J.-H. Lee, and S. Lee (2003), Structure and eastward extension of the Changjiang River plume in the East China Sea, J. Geophys. Res., 108, JC001194.

Milliman, J. D., S. Huang-Ting, Y. Zuo-Sheng, and R. H. Meade (1985), Transport and deposition of river sediment in the Changjiang estuary and adjacent continental shelf, Cont. Shelf Res., 4, 37-45.

Moon, J.-H., I.-C. Pang, Jong, and J.-H. Yoon (2009), Response of the Changjiang diluted water around Jeju Island to external forcings: A modeling study of 2002 and 2006, Cont. Shelf Res., 29, 1549-1564.

Moore, W. S. and R. Arnold (1996), Measurement of ^{223}Ra and ^{224}Ra in coastal waters using a delayed coincidence counter, J. Geophys. Res., 101, 1321-1329.

Moore, W. S. (2000), Determining coastal mixing rates using radium isotopes, Cont. Shelf Res., 20, 1993-2007.

Moore, W. S. and J. Krest (2004), Distribution of ^{223}Ra and ^{224}Ra in the plumes of the Mississippi and Atchafalaya Rivers and the Gulf of Mexico, Mar. Chem., 86, 105-119.

Nozaki, Y. (1989), Mean residence time of the shelf water in the East China and the Yellow Seas determined by ^{228}Ra/^{226}Ra measurements, Geophy. Res. Lett.,

16, 1297-1300.

Nozaki, Y., H. Tsubota, V. Kasemsupaya, M. Yashima, and N. Ikuta (1991), Residence times of surface water and particle-reactive ^{210}Pb and ^{210}Po in the East China and Yellow Seas, Geochim. Cosmochim. Acta, 55, 1265-1272.

Scholten, J. C., M. K. Pham, O. Blinova, M. A. Charette, H. Dulaiova, and M. Eriksson (2010), Preparation of Mn-fiber standards for the efficiency calibration of the delayed coincidence counting system (RaDeCC), Mar. Chem., 121, 206-214.

Sun, Y. and T. Torgersen (1998), The effects of water content and Mn-fiber surface conditions on ^{224}Ra measurement by ^{220}Rn emanation, Mar. Chem., 62, 299-306.

Tsunogai, S., S. Watanabe, J. Nakamura, T. Ono, and T. Sato (1997), A preliminary study of carbon system in the East China Sea, J. Oceanogr., 53, 9-17.

Waska, H., S. Kim, G. Kim, R. N. Peterson, and W. C. Burnett (2008), An efficient and simple method for measuring ^{226}Ra using the scintillation cell in a delayed coincidence counting system (RaDeCC), J. Environ. Radioact., 99, 1859-1862.

Webster, I. T., G. J. Hancock, and A. S. Murray (1995), Modelling the effects of salinity on radium desorption from sediments, Geochim. Cosmochim. Acta, 59, 2469-2476.

Wells, J. T. (1988), Distribution of suspended sediment in the Korea Strait and southeastern Yellow Sea: onset of winter monsoons, Mar. Geol., 83, 273-284.

Wong, G. T. F., G.-C. Gong, K.-K. Liu, and S.-C. Pai (1998), 'Excess Nitrate' in the

East China Sea, Estuar. Coast. Shelf Sci., 46, 411-418.

Zhang, J. (2002), Biogeochemistry of Chinese estuarine and coastal waters: nutrients, trace metals and biomarkers, Reg. Environ. Change., 3, 65-76.

Zhang, L., Z. Liu, J. Zhang, G. H. Hong, Y. Park, and H. F. Zhang (2007), Reevaluation of mixing among multiple water masses in the shelf: An example from the East China Sea, Cont. Shelf Res., 27, 1969-1979.

6. Korean Abstract

동중국해, 남해, 그리고 황해를 포함하는 북서태평양 주변해 표층수 중 ^{223}Ra과 ^{228}Ra 농도의 수평적 분포를 이용하여 양자강희석수(CDW)의 흐름속도 및 주변 해수와의 상대적 혼합비율을 계산하였다. 수평적인 ^{223}Ra 농도의 분포를 이용하여 구한 양자강 하구에서 북동쪽 방향 450km까지의 양자강희석수의 유속은 16 ± 1 cm/s였고, 이 결과값은 표류부이, 수치모델 등 물리적 방법을 이용한 결과값과 유사하였다. 또한, 염분과 ^{228}Ra의 물질수지 방정식을 이용하여 각 정점에서 양자강희석수의 상대적 혼합비율을 계산하였다. 양자강희석수의 혼합비율은 동중국해 북부와 황해 대부분 해역의 표층에서 50% 이상이었고, 심지어 강으로부터 약 800 km 떨어진 대한해협의 표층까지 약 30%의 분포를 보였다. 이러한 결과는 여름철 양자강희석수가 북서태평양 주변 표층해수의 생지화학적 과정에 매우 중요할 수 있음을 의미한다.

주제어: 라듐 동위원소; 양자강 희석수(CDW); 유속; 수괴혼합

학번: 2012-22511

7. Acknowledgement

군인으로서의 삶을 살아오던 저에게 이곳 서울대학교에서의 2년 간의 생활은 또 다른 도전이자 시련의 연속이었습니다. 연구의 기본 개념조차 알지 못했던 저를 지금에 오기까지 이끌어주시고 지도해주신 김규범 교수님께 깊은 감사의 말씀을 드립니다. 또한, 논문심사를 맡아주시고 저의 부족한 점을 지도해주신 서울대 조양기 교수님과 이강근 교수님께도 감사 드립니다. 해양학이라는 학문의 길로 들어서는 첫 발을 내딛게 해주신 해군사관학교 교수부장 송기훈 교수님, 박경주 교수님, 임세한 교수님, 길범준 교수님, 그리고 첫 학기 저의 청강요청을 흔쾌히 허락하시며 많은 가르침을 주신 이창복 교수님, 항상 반갑게 맞아주시고 격려를 해주신 해양연구소 윤재열 박사님, 연구실 대 선배님으로 격려와 응원을 아끼지 않으신 국립수산과학원 황동운 박사님, 그리고 해양환경관리공단 이용우 박사님, 동중국해 해양관측 때 세세한 관심으로 챙겨주셨던 국립수산과학원 박성은 박사님께도 감사 드립니다.

연구실 큰 형님으로서 학문적 분야의 조언뿐만 아니라 첫 서울 생활을 잘 적응하는데 많은 도움을 주신 태훈 형, 힘들 때마다 얘기를 들어주시고 함께 고민해주신 정 많은 용화 형, 학문적 성장을 이루는데 도움을 주신 인태 형, 논문작성에 적극적으로 도와주신 정현 형, 잘 하고 있다며 응원해준 Ge Yan 형, 멀리 미국에서 관심과 조언을 해주셨던 종선이형, 그리고 후배이지만 연구에 많은 조언을 해줬던 유식에게도 진심으로 감사 드립니다. 또한, 실험실에서 동고동락했던 형미와 신아, 졸업 때문에 걱정 많으신 정현 누나, 그리고 막내 재홍이까지 함께할 수

있어 행복했습니다. 곁에서 학문적 조언뿐만 아니라 많은 격려와 용기를 북돋아 줬던 경하, 무뚝뚝한 것 같지만 마음은 따뜻한 광일 형, 늘 예의 바르고 성실한 가희, 만날 때마다 안부 물어봐 주시는 마음씨 착한 명택 형, 동해 관측조사에서 함께 동고동락했던 민호, 승태, 그리고 재암 형에게도 감사 드립니다.

마지막으로 지금의 저를 있게 해주신 아버지와 어머니, 그리고 항상 동생을 응원해주는 누나에게도 감사 드립니다. 2005년 1월 5일 수능 실패 후 재수하겠다고 무작정 집을 떠났던 것이 벌써 9년이란 시간이 흘렀습니다. 다른 동기들처럼 집을 떠나 동해, 남해, 서해를 홀로 떠돌며 아들로서 그 동안 못다한 시간들은 앞으로 살면서 채워나가겠습니다.